EFDA–JET–PR(12)43

R. Neu, G. Arnoux, M. Beurskens, V. Bobkov, S. Brezinsek, J. Bucalossi,G. Calabro, C. Challis, J.W. Coenen, E. de la Luna, P. C. de Vries, R. Dux, L. Frassinetti, C. Giroud, M. Groth, J. Hobirk, E. Joffrin, P. Lang, M. Lehnen, E. Lerche, T. Loarer, P. Lomas, G. Maddison, C.F. Maggi, G. Matthews, S. Marsen, M. Mayoral, A. Meigs, Ph. Mertens, I. Nunes, V. Philipps, T. Pütterich, F. Rimini, M. Sertoli, B. Sieglin, A.C.C. Sips, D. van Eester, G. van Rooij and JET EFDA contributors

First Operation with the JET ITER-LikeWall

First Operation with the JET ITER-LikeWall

R. Neu[1,3], G. Arnoux[2], M. Beurskens[2], V. Bobkov[3], S. Brezinsek[4], J. Bucalossi[5], G. Calabro[6], C. Challis[2], J.W. Coenen[4], E. de la Luna[7], P.C. de Vries[8], R. Dux[3], L. Frassinetti[9], C. Giroud[2], M. Groth[10], J. Hobirk[3], E. Joffrin[5], P. Lang[3], M. Lehnen[4], E. Lerche[11], T. Loarer[5], P. Lomas[2], G. Maddison[2], C.F. Maggi[3], G. Matthews[2], S. Marsen[12], M. Mayoral[1], A. Meigs[2], Ph. Mertens[4], I. Nunes[13], V. Philipps[4], T. Pütterich[3], F. Rimini[2], M. Sertoli[3], B. Sieglin[3], A.C.C. Sips[14], D. van Eester[11], G. van Rooij[8] and JET EFDA contributors*

JET-EFDA, Culham Science Centre, OX14 3DB, Abingdon, UK

[1]EFDA-CSU, Boltzmannstr.2, 85748 Garching, Germany
[2]EURATOM-CCFE Fusion Association, Culham Science Centre, OX14 3DB, Abingdon, OXON, UK
[3]Max-Planck-Institut für Plasmaphysik, EURATOM Association, Boltzmannstr.2, 85748 Garching, Germany
[4]IEK-4,Association EURATOM/ForschungszentrumJülich GmbH 52425, Germany
[5]IRFM-CEA, Centre de Cadarache, 13108 Saint-Paul-lez-Durance, France
[6]Associazione EURATOM-ENEA sulla Fusione, CNR ENEA Frascati, 00044 Frascati, Italy
[7]Laboratorio Nacional de Fusion, Asociation EURATOM CIEMAT, Madrid, Spain
[8]Association EURATOM/DIFFER, Rijnhuizen PO Box 1207 3430BE Nieuwegen, Netherlands
[9]Association EURATOM-VR, Division of plasma physics, KTH, Stockholm, Sweden
[10]Association EURATOM-Tekes, Aalto University, Finland
[11]Association EURATOM-Etat Belge, ERM-KMS, Brussels, Belgium
[12]Max-Planck-Institut für Plasmaphysik, EURATOM Association, Wendelsteinstr. 1, 17491 Greifswald, Germany
[13]Institute of Plasmas and Nuclear Fusion, Association EURATOM-IST, Lisbon, Portugal
[14]EFDA-CSU, Culham Science Centre, OX14 3DB, Abingdon, UK
** See annex of F. Romanelli et al, "Overview of JET Results", (24th IAEA Fusion Energy Conference, San Diego, USA (2012)).*

Preprint of Paper to be submitted for publication in
Physics of Plasmas

ABSTRACT.
To consolidate ITER design choices and prepare for its operation, JET has implemented ITER's plasma facing materials, namely Be at the main wall and W in the divertor. In addition, protection systems, diagnostics and the vertical stability control were upgraded and the heating capability of the neutral beams was increased to over 30 MW. First results confirm the expected benefits and the limitations of all metal plasma facing components (PFCs), but also yield understanding of operational issues directly relating to ITER. H-retention is lower by at least a factor of 10 in all operational scenarios compared to that with C PFCs. The lower C content (Section 1factor 10) have led to much lower radiation during the plasma burn-through phase eliminating breakdown failures. Similarly, the intrinsic radiation observed during disruptions is very low, leading to high power loads and to a slow current quench. Massive gas injection using a D_2/Ar mixture restores levels of radiation and vessel forces similar to those of mitigated disruptions with the C wall. Dedicated L-H transition experiments indicate a reduced power threshold by 30%, a distinct minimum density and pronounced shape dependence. The L-mode density limit was found up to 30% higher than for C allowing stable detached divertor operation over a larger density range. Stable H-modes as well as the hybrid scenario could be only re-established when using gas puff levels of a few 10^{21} es^{-1}. On average the confinement is lower with the new PFCs, but nevertheless, H factors up to 1 (H-Mode) and 1.3 (at $\beta_N \approx 3$, hybrids) have been achieved withWconcentrationswell below themaximum acceptable level.

1. INTRODUCTION

Plasma wall interaction (PWI) research and development has become a priority for the international fusion community because of the huge extrapolation necessary in terms of particle fluence and transient power loads when progressing to next step devices such as ITER or DEMO. In response, the ITER-like wall (ILW) project was initiated at JET [1, 2] using beryllium (Be) as first wall and tungsten (W) as divertor armour material, mimicking the ITER choice of plasma facing materials (PFMs) during its active phase [3]. The experiments at JET with its ILW (JET-ILW) started in summer 2012, providing the unique opportunity to address specific issues related to the parallel use of Be andWas PFMs with plasma parameters closest to those of ITER. Amongst these are the investigation of fuel retention compared to a carbon device, the test of ITER relevant conditioning procedures, mixed materials effects, W erosion and transport in ITER relevant scenarios (baseline and advanced), the effect of ELMs and ELM mitigation methods as well as the behaviour of melt layers under steady state and transient heat loads.

In order to keep the implementation of the ILW manageable, the impact of the materials changes on JET operational limits and work with the existing support structures had to be minimized. In themain chamber this was achieved by using bulk berylliumon Inconel carriers for the limiters and with tungsten coated CFC [4] in some higher heat flux recessed areas, for example the neutral beam shine through areas, and beryllium coated Inconel elsewhere [5]. The divertor consists ofW-coated

CFC tiles [6] and a single toroidally continuous belt of bulk tungsten at the outer strike point [7]. Besides this obvious reconstruction a large amount of details had to be changed/optimized [8] as for example the upper dump plate now consists of bulk Be ribs with beryllium coated Inconel plates between, rather than a continuous sheet of tiles. The anticipated operating limits with the ILW are most fundamentally driven by the relatively low melting point of beryllium (1629 K), the limited robustness of tungsten coatings to slow and fast thermal cycles and the thermal capabilities of the support structures for the bulk tungsten tile [9].

The protection of the ILW was an integral part of the project from very early on. In order to achieve PFC temperature measurements in real time, a comprehensive set of bicolour pyrometers (8) and monochrome video cameras (7) with adjustable filters and thermocouples was installed. Together with the appropriate software a fast reaction of the discharge control has been possible and a detailed map of the energy deposition on the PFCs could be established [10].

2. OPERATIONAL EXPERIENCE WITH THE JET ITER-LIKE WALL

2.1. PLASMA BREAKDOWN

The ITER-like wall was found to have a profound impact on plasma breakdown [11]. As expected, the avalanche phase was unaffected and seems to be dominated by the pre-fill pressure and its composition, but the burn-through phase strongly depends on the plasma facing material. The recycling or out-gassing properties and the levels of main impurities such as carbon changed significantly with the introduction of the ITER-like wall, affecting the density and radiation in the burn-through phase. The highest radiation levels during the burn-through phase were obtained at the start of the ILW operation, when the carbon levels were still higher, but also during and after the use of N as extrinsic impurity in experiments for radiative cooling. The lower radiation efficiency of beryllium in comparison to carbon in combination with the fact the peak radiation is at lower temperature, allows for a faster burn-through. For the carbon wall, out-gassing and impurity release were responsible for a large part of the electron density build up during the burn-through phase. In contrast, this component was almost absent with the ITER-like wall and the density was determined by the amount of pre-fill gas making it more reproducible and successful plasma burn-through could be achieved with higher pre-fill pressures and higher densities. The higher dynamic retention with the ITER-like wall made it however more difficult to sustain the neutral and plasma density which in turn may have complicated low voltage breakdown (Mode B) for which the Townsend avalanche criteria [11] allow only a limited pre-fill pressures range. Independently, the changes in breakdown with the ITER-like wall did not lead to a substantial reduction in flux-consumption.

The plasma burn-through including plasma-surface interaction effects has been self-consistently modelled [12]. The simulations show that with a carbon wall chemical sputtering allows the carbon content to build up during the formation of the plasma, dominating the radiation. In contrast the model shows that physical sputtering of beryllium does not raise radiation levels much above those obtained with pure deuterium plasmas, similar as seen in the experimentally.

As a consequence of this very beneficial behavior of the plasma break down no overnight glow discharges and no Be evaporation were necessary in contrast to the experience with carbon walls. Note that there were only two Be-evaporations in the first year of operation in order to investigate their influence on the impurity production by ICRH.

2.2. IMPURITY SOURCES AND CONTENT

Monitoring pulses were introduced to the routine plasma operations of JET-ILW [13] and typically performed once a week, in order to allow tracking the evolution of the machine performance and intrinsic impurities throughout the 2011/2012 campaigns. After the initial restart of JET-ILW about 300 JET Pulses (2000s) of divertor operation were required to establish a steady state divertor composition [14]. Throughout the whole campaigns only a moderate increase (≤20%) of the carbon influx from the inner divertor is found. This observation is attributed to the fact that although the monitoring pulses were performed always identical, the energy input into the plasma discharges in between the monitoring discharges was continuously rising throughout the campaigns probably mobilising residual carbon. In this context it has to be noted that no macroscopic failure of the W coatings was detected by regular video inspections of the vessel interior so far as well as in a first assessment after the surfaces during the ongoing vent. Fig.1 shows a compilation of Z_{eff} values and normalised main chamber carbon influxes (CIII/n_e) for all discharges throughout the ILW campaigns as well as from the previous campaigns with theMK HD CFC divertor. Carbon drops by a factor of about 20 and at the same time the averaged Z_{eff} drops from 1.96 to 1.21 [15]. Assuming C as main intrinsic impurity in JET-C and Be in JET-ILW respectively, an averaged carbon concentration of ≈3% and an averaged beryllium concentration of 2% can be deduced, in line with typical concentration deduced from charge exchange spectroscopy (CXS). The CXS also shows C concentrations in the ILW well below 0.5%. As with the C influx from the divertor, the C influx in the main chamber shows a clear increase towards the end of the first year of operation. This increase is strongly correlated with the increased energy throughput stated above and shows a very similar correlation with power as in JET-C, albeit at a factor of 10 lower levels [15]. Due to the strong gettering effect of Be, oxygen is strongly supressed and despite an evident vacuum leak, its level at the beginning of the JET-ILWcampaigns is as low as in JET-C after months of operation and many Be evaporations.

Passive spectroscopy was used for the characterisation of the erosion at the solid Be limiters using the inverse photon efficiency (the so called S/XB-value) [16]. In order to calculate an ”effective” erosion yield the peak Be particle flux densities were normalized to the saturation current measured by Langmuir probes mounted on the reciprocating probe evaluated at the same radial position. This is a common practice, to express that the majority particle (deuterium) is not the the only sputtering particle, but also other intrinsic impurities or self-sputtering are contributing to the yield. Effective yields of up to 10% were observed for a wide range of plasma parameters in a series of limiter discharges specifically performed for an erosion study [17].

The W erosion in the JET outer divertor was evaluated as a function of the divertor electron temperature in L-mode and H-Mode discharges again by means of visible spectroscopy [18]. The W influx was deduced from a transition at 400.9nm in neutral tungsten (W I) and the temperature dependent S/XB-value was taken from a recent compilation [19] of theoretical and experimental data from different devices.

In the investigated L-Mode discharges (1 MW of NBI heating) the effective erosion yield increases monotonically with divertor temperature up to $\approx 5 \cdot 10^{-4}$ at $T_e = 45$eV and for the lowest value of $T_e \approx 7$eV achieved in a density scan, a steep decrease of the effective erosion yield below 10^{-6} is found, revealing the threshold behaviour expected for W sputtering dominated by Be^{2+} ions. Indeed there is good agreement of effective erosions yields with calculated sputter yields assuming a 0.5% Be fraction in the divertor plasma, which is consistent with spectroscopic measurements of the Be influx [18]. It has to be noted however that at low line averaged plasma densities ($n_e \leq 2 \cdot 10^{19}$ m^{-3}) and ICRH power up to 3MW, effective erosion yields > 10^{-3} are measured at divertor temperatures above 50eV, pointing to a higher fraction of impinging Be-ions.

In H-Mode discharges, a large difference between inter- and intra-ELM W sputtering is observed. In a discharge heated with 13MW of NBI, with $n_e = 7.5 \cdot 10^{19}$ m^{-3} and 10Hz ELMs, a W influx of 6.3 · 1018 W s−1 and an effective inter-ELM sputter yield of $4 \cdot 10^{-5}$ was found, thus being similar to the L-mode sputter yields given above. The intra-ELM sputtering measurement for this case gave a W source of $4.7 \cdot 10^{18}$ W/ELM. Given the 10Hz ELM frequency, this means that intra-ELM sputtering dominated by a factor of 8 over the inter-ELM sputtering similar to observations in ASDEX Upgrade [20].

Nitrogen seeding has been used for reducing power and energy loads on divertor targets by radiative cooling (see Sec.3.5). As long as the cooling is not efficient enough an increase of the W influx is expected with the increased N influx. This effect was investigated in L-mode discharges with 1.1MW heating power from NBI and N_2 seeding rates $4 \cdot 10^{21}$ $1 \cdot 10^{22}$ es^{-1}). A maximum effective erosion yield is observed around a divertor temperature of $T_e = 20$eV, i.e. here the effect of plasma cooling started to dominate and nitrogen seeding had a net beneficial effect on the W erosion when the divertor temperature decreased below 15eV.

In Fig.2 the impact of equal amounts of auxiliary heating (3.5MW) applied by either ICRH (Ion Cyclotron Resonance Heating) or by NBI (neutral beam injection) are presented, while ensuring the density is the same (central line integrated density $\approx 6 - 7 \cdot 10^{19}$ m^{-2}) [21]. The radiation level during ICRH is larger by a factor of 3 and most radiation originates from the bulk while the radiation for beam heating is mainly concentrated in the divertor region (Fig.2d). The W concentration in the plasma was evaluated from VUV spectroscopy [22] allowing some radial resolution by using emissions from distinctly different ionisation states. The W concentration is strongly increased during ICRH, explaining the entire increase of the radiation. The ratio between the edge and core W concentrations measured by spectroscopy (Fig.2c) and the high central temperatures achieved during ICRH (Fig.2b) suggest that the W density profile is hollow, pointing to the beneficial effect

of central ICRH in respect the suppression of W accumulation as already observed in AUG [23] and in JET for Ni [24]. This observation is corroborated by tomographic reconstruction of bolometric measurements which show an off-axis peaked radiation pattern. Nevertheless, the strong increase of the W content was unexpected because the antenna limiters are completely made out of Be. Moreover no significant increase of the W source in the divertor, neither at the strike point region nor at the baffle at the divertor entrance was observed, leaving the source yet unidentified [25]. In principle, a change in the (edge) transport could also lead to a higher W concentration, but this seems to be unlikely because copper, which is detected as a trace impurity, does not increase during ICRH. In order to shed more light on potential source, two beryllium evaporations were performed towards the end of the campaign. This resulted in a reduction by almost a factor of 2 of the total radiation during ICRH, which lasted formore than 10 discharges. Since the W divertor sources recovered much faster after the Be evaporations than the high Z content of the main plasma, one can conclude the the additional W (and Ni) sources during ICRH must not be located in areas with large particle fluxes. Indeed, tungsten surfaces exist in recessed areas in the main chamber at the high field side as well as at the low field side [8], but the detailed mechanism how the plasma can reach this areas during ICRH has still to be assessed.

2.3. DISRUPTION BEHAVIOUR

The ITER-like Wall had a significant impact on disruption physics at JET [26]. The strongreduction of the C concentration seen from the very first ILW discharges had two direct consequences. Firstly, the onset of the disruptive density-limit, the MARFE development, occurs at lower divertor temperatures, well below the optimum temperature for C radiation, and thus it is possible to achieve higher line-averaged plasma densities [27]. Secondly, lower radiation and hence higher temperatures are observed during unmitigated ILW disruptions as can be seen in Fig.3. This lengthened the current quench phase, increasing the impulse by the electromagnetic disruption force on the vessel. Moreover, a larger fraction of the total energy being conducted to the Be wall which is vulnerable to melting [26]. Because of the larger vessel forces and heat loads, active mitigation by massive gas injection (MGI) became a necessity for ILW operations. For the first time it has been applied as an active protection system at JET.

In Fig.3 it can be seen that MGI is capable of increasing the radiation fraction close to 100% , thus significantly reducing the fraction of energy conducted to the PFCs and reducing the current quench duration. On the positive side, the longer current quench rates and thus lower toroidal electric fields have made it more difficult to generate runaway electron beams [28]. Disruptions with the ILW, unmitigated and even those mitigated by MGI, were found to have a negligible impact on the following discharge. So far no cases have been found where the plasma formation failed because of de-conditioning due to disruptions.

2.4. FUEL RETENTION

Global gas balance experiments have been performed throughout the first campaigns starting with

ohmic plasmas in the initial phase of divertor operation and finishing with NBI heated H-mode plasmas at the last day of operation. The short term retention, studied in-situ by investigating the gas puff levels and neutral pressures, increases in the limiter plasma phase with the Be first wall. However, the outgassing after the discharge over compensates this transient retention [29]. The long term retention, i.e. the number of retained deuterium ions in the first wall components per second, has been deduced taking into account the amount of injected D through the gas injection systems and, if applicable, the neutral beam injection, and the number of actively pumped neutrals by the applied pumping systems. The pumped gas is collected by the JET active gas handling system (AGHS), quantified by calibrated pressure measurements, and analysed for its components by gas chromatography [30, 31]. All experiments were carried out in series of comparable repetitive discharges, minimum 9 and maximum 34 consecutive plasmas, until the number of injected particles reached approximately the analysis limit of the AGHS maximising the plasma exposure and minimising the impact of history effects. The retention rates were obtained by normalising to the integrated plasma time in divertor configuration reflecting the plasma time with the main ion flux interaction with the divertor PFCs. In order to compare with previously performed reference discharges in JET-C [32], the discharges with the ILWwere adapted in input power, magnetic configuration and fuelling rate to match edge plasma conditions, i.e. the density and deuterium ion flux, of CFC references as closely as possible. Apart from the material comparison, the fuelling rate ($1 \cdot 10^{21}$ Ds^{1} $1 \cdot 10^{23}$ Ds^{1}), also the auxiliary heating ($P_{aux} = 0$ 12.0MW), as well as the ion flux to the divertor ($\Gamma_{ion} = 2 \cdot 10^{22}$ m^2 s^{-1} $2 \cdot 10^{23}$ m^2 s^{-1}) were varied. All JET-ILW experiments showed low retention rates covering a range of 2 $16 \cdot 10^{19}$ Ds^{-1} applying the same analysis as in JET-C and showed high purity of the recovered gas of more than 99.0% D. In L-Mode as well as in H-Mode a reduction of the retention by at least a factor of 10 is deduced which confirms qualitatively the predicted reduction of fuel retention in ITER with Be first wall and W divertor compared with a hypothetical full carbon ITER described in comprehensive studies [33]. The most likely mechanism for the remaining fuel retention in the JET-ILW experiments is co-deposition of fuel in Be-layers which is in line with the measured high Be influx from the main chamber into the inner divertor leg whose plasma-facing surfaces are a net deposition zone. PISCES studies of fuel content in Be layers showed a ten times lower D content than C layers at 200 C [33] which can explain the observed reduction. Co-deposition with W is not of importance and implantation is the main mechanism for the retention in W as experiments in ASDEX Upgrade confirmed [34], but it plays itself a negligible role in comparison with the Be co-deposition. Long-term outgassing also observed in JET-C, but being of minor importance due to the higher absolute retention [35], has also been observed in JET-ILWfor about 100h after plasma pulses with the deuterium pressure decaying according to $\sim t^{-0.8}$ [29] which will lead to a further substantial reduction of the fuel content in the metallic PFCs. Therefore it is expected that the post mortem analysis of Be andWcomponents will show a significant lower long term fuel content as deduced from the gas balances. The tiles will be retrieved from the vessel during the current vent end of 2012.

3. H-MODE PHYSICS IN AN ALL-METAL ENVIRONMENT

3.1. L-H POWER THRESHOLD

Dedicated experiments have been carried out to investigate the L-H power threshold in JETILW, with I_p/B_t and plasma shape matched to those within the JET-C [36]. The plasma density was varied from discharge to discharge and slow input power ramps (ICRH or NBI), typically 1 MW/s, were used to measure P_{thr}. In JET-C, at $B_t = 1.8T$, $I_p = 1.7MA$, the threshold power P_{thr} defined as heating power reduced by dW/dt was found to be consistent with the multi machine scaling law $P_{thr,08}$ [37]. Conversely, in density scans with the ILW both P_{thr} and $P_{sep} = P_{thr}P_{rad,bulk}$ (the bulk radiated power) increase below a minimum density, $n_{e,min} \approx 2.2 \cdot 10^{19}$ m^{-3} thus recovering the low density behaviour observed with MkII-GB divertor (C wall) as well as in the all metal devices Alcator C-Mod [38] and ASDEX Upgrade [39]. At plasma densities above ne,min, P_{thr} is reduced by ≈30%and P_{sep} by ≈40% in JET-ILWcompared to JET-C. A similar reduction of the H-mode threshold has been found in ASDEX Upgrade comparing operation with carbon PFCs to that with tungsten PFCs [40]. The strong influence of the wall change from C to Be/W on P_{thr} and P_{sep} is also observed at 3.0T/2.75MA and ne,min increased roughly linearly with Bt, being unfavourable for ITER, which needs to access the H-mode at high magnetic field ($B_t = 5.4T$). At given edge density, the L-H transition occurs at lower edge electron temperature, Te,edge with the ILW. In NBI heated discharges, where the ion temperature $T_{i,edge}$ can be measured by edge charge exchange spectroscopy, $T_{i,edge}$ and $T_{e,edge}$ are found to be strongly coupled over the explored density range.

3.2. BASELINE H-MODE SCENARIO

In order to allow the reliable and safe operation in high power H-Modes special emphasis was dedicated to the H-Mode scenario development. The main elements were the establishment of a stable current ramp up phase, the avoidance of large ELMs at the entry of the H-mode phase, the optimisation of confinement in the flattop phase and finally the save exit from HMode and discharge landing - always staying within the material limits given by the metallic wall [41]. Stable Type I ELM sawteething H-modes have been achieved for 4 to 5s (duration of main heating phase) in low and high plasmas, initially at 2.0MA/2.1T and then at 2.5MA/2.7T with $q_{95} = 3.5$ and above 20MW of auxiliary power (see Fig.4). It became clear that deuterium had to be puffed at a significant rate (above 10^{22} Ds^{-1}) in the divertor during the main heating phase to achieve stable conditions with respect to central radiation peaking as already shown in ASDEX Upgrade [40]. By increasing the puff rate the ELM frequency increased and a minimum ELM frequency of typically 10Hz or more was necessary to prevent excessive core plasma radiation arising from W and Ni, which could lead to a back transition to L-mode as the power crossing the separatrix decreases. In this situation, the sawtooth activity did not seem to prevent radiation peaking and even vanished as the temperature became hollow (see Sec.3.4). In general, no disruption occurred if the auxiliary heating was maintained, whereas switching off the NBI power in such a case could lead to disruption by radiation collapse event. The increase of the NBI power combined with strong deuterium gas puffing

rate (above 10^{22} Ds^{-1}) opened up the operating space by increasing central transport and the ELM frequency and therefore the flushing out tungsten from the bulk plasma (see also Sec.3.4), as seen in AUG [42, 43]. Since both the increase of the loss power (power crossing the separatrix) and the gas puffing contribute to expell tungsten by increasing the ELM frequency, it was also found that the minimum gas puffing rate decreases with the loss power. However, the high gas puffing rate deteriorated also the confinement of the H-mode. At high triangularity ($\delta \approx 0.4$) the H-mode scenario shows a confinement degradation by 10 to 30% with gas puffing which was not observed with the C-wall at a similar level of gas fuelling [44]. For the lowest fuelling cases, the confinement factor H98 approached sometimes 1 indicating that the H = 1 access is possible at $I_p \leq 2.5$MA (without strong central heating). In an attempt to open up this space, vertical kicks [45] have been applied to control the ELM frequency. Although the ELM frequency could indeed be controlled at about 30Hz and the gas rate could be reduced down to $5 \cdot 10^{21}$ Ds^{-1}, the Hfactor could not yet be restored to values closer to 1, hinting to another necessary ingredient responsible for the reduced confinement.

Part of the scenario development in JET-ILW was also devoted to the adaptation of the Hmode termination and discharge landing. Because with the ILW the W could accumulate and radiate from the plasma core, switching off the power at termination often resulted in a radiative collapse. This may be explained by the longer residence time of heavy impurities in the plasma than that of light impurities. The use of electron heating (typically ≈ 2MW of ICRH) in the landing phase was successful in avoiding disruptions. In this phase, the electron temperature could be increased up to 6 or 7keV and helped in preventing the radiation collapse.

On the basis of the initial low triangularity ($\delta = 0.2$) H-mode development at 2.5MA/2.7T ($q_{95} = 3.5$), the baseline operational domain was extended up to 3.5MA/3.2T ($q_{95} \approx 3$). Large gas injection was intentionally used again to stabilise the discharge keeping the ELM frequency above ≈10–20Hz. Strike point sweeping of about ±6 cm was successfully applied on the bulk tungsten tile to keep the surface temperature at the tile below 1200°C. Using this cautious approach, plasmas were successfully developed at $\beta_N \approx 1.4$ with 25MW of NBI power for more than 5s duration and a Z_{eff} of 1.2-1.3. ICRH power was also coupled successfully up to a level of 3.5MW during the flattop. An elevation of the core temperature and larger sawtooth activity were clearly observed in the ICRH phase but there was no clear evidence yet that it had a beneficial effect on the high Z impurity core concentration. In comparison to the C-wall high current scan with the same triangularity, the confinement is consistently lower by 20 to 30% at same the plasma current, q_{95} and shape. Attempts to recover the confinement by lowering the gas injection down to a rate of $2 \cdot 10^{22}$ Ds^{-1} and increasing the heating power to provide P_{loss}/P_{th} well above 2 while keeping the ELM frequency above 10Hz, have not succeeded in recovering more than 10% of the confinement. As a result, the ρ^* and ν^* are still higher by typically 50% and 30% respectively than with the C-wall.

3.3. HYBRID H-MODE SCENARIO

The hybrid scenario has also been developed using as references the work carried out in JETC

[46]. This scenario is traditionally characterised by its access to high normalised pressure ($\beta_N >$ 2.5) and no or infrequent sawteeth activity due to its 'broad' q-profile shape. The latter is achieved in JET by using the current overshoot technique which helps keeping the central target q value (q_0) close to unity and maximising the amount of current density at midradius. As already found in the baseline scenario, more gas had to be injected in the early phase of the discharge compared to the experiments in JET-C to achieve the same plasma density although the X-point is already formed after 1.4s. Too low gas injection resulted in the creation of a run-away electron population and an increased tungsten level. With increased gas injection, the early q profile at the X-point formation was much lower in the plasma core (typically 3 or 4 instead of 6 or 7 as measured by Motional Stark Effect, MSE) than it was with the C-wall. Using this I_p overshoot technique, the hybrid scenario has been developed at low δ ($\delta \approx 0.2$–0.3) and high δ ($\delta \approx 0.4$) for $q_{95} \approx 4$ at 1.4–1.7MA/2.0T and 1.7–2.0MA/2.3T [41]. In all discharges, the outer strike point was located on the horizontal divertor bulk tungsten tile (with the C-wall the plasma configuration had a more outward strike point position closer to the pumping louvers). In these attempts the hybrid scenario could be reproduced showing for about 2 to 3 s similar global performance (H98 = 1.1–1.3 with $\beta_N \approx 3$) as achieved in the C-wall at both high and low triangularity, however for the low triangularity at higher density and lower temperature. For both triangularities moderate gas fuelling ($\approx 5 \cdot 10^{21}$ Ds^{-1}) was required to keep the discharge stable with regard to core radiation. The hybrid scenario with the ILW had in general similar m = 1, n = 1 fishbone activity as with the C-wall. However, unlike the experiments in JET-C, continuous m = 1, n = 1 modes sometimes developed leading to a significant reduction of confinement [47]. Similarly, the m = 3/n = 2 and m = 4/n = 3 MHD activities were also observed, leading to a slow decrease of central electron temperature and an enhanced radiation from the plasma core. This is in contrast to observations with the C-wall where such events could be recovered from and did not terminate the discharge in radiative collapse.

The difference in performance between the hybrid and the baseline H-modes is quite obvious but the reasons for this are not yet understood, even though part of the improved performance can be attributed to better core confinement (see Sec. 3.6). A possible explanation could be that higher confinement is preferably achieved at higher β-values or at an operation further above the L-H threshold (2–3.5 instead of 1.5–2.0 used in the baseline scenario) as there are also hints for this from ASDEX Upgrade [48]. Additionally, the hybrid H-mode scenarios are not run with the same I_p, B_t and q_{95} as the baseline scenarios and heating deposition and the radiation profiles may be different in these two scenarios.

3.4. W ACCUMULATION

In discharges where too much W enters the plasma core, W accumulation can develop, strongly impacting on the core plasma parameters and the confinement. Figure 5 shows an H-mode discharge with an ELM-frequency of 10–15Hz, exhibiting the typical behaviour of slow W accumulation. From t = 9.0s on the deuterium gas puff is lowered to $5 \cdot 10^{21}$ s^1. Up to t = 11.5s the diamagnetic

energy (Wdia) does not considerably change, while the radiated power in the main chamber (P_{rad}) continuously increases. Similarly, the core electron temperature (T_e) as measured by electron cyclotron emission (ECE) decreases, while the edge values stay constant (Fig.5(b)). During the same period the electron density (n_e) (Fig.5(c)), as measured by Thomson scattering, keeps rising in the plasma core and the edge values stay constant, which implies that the density starts peaking. Only after t = 11.5s the core Te collapses drastically and a steep increase of P_{rad} is observed affecting Wdia and correspondingly the H98-factor (Fig.5(d)). As the line averaged $Z_{eff} \approx 1.2$ does not strongly change during the rise of the radiation, medium to high-Z elements must be causing it. However, the W-concentration (c_W) as measured by the spectrometer stays constant through out. In order to estimate the radiated power due to W, the W-concentration, which is locally measured at a certain radial range, is assumed to apply for the full plasma volume - this estimate is depicted in 5(a) and labeled est. W-rad. The W-radiation seems to be negligible during all phases of the discharge and thus seems to indicate that W may not be responsible for the rise of the main chamber radiation. However, the spectrometer line of sight is vertical and may be missing parts of theWemissions because of poloidal asymmetries that arise from centrifugal forces. Additionally, the measured W spectral lines in the VUV spectral range yield information from a limited radial region only [22]. This interpretation is confirmed by SXR emission profiles revealing poloidal asymmetries, which can be described as a consequence of centrifugal forces acting on strongly rotating W ions [49] as described earlier in the case of nickel by Wesson [50]. The asymmetries show up most clearly just outside of the sawtooth inversion radius. Since strong contributions to the SXR signal from other intrinsic impurities can be excluded by auxiliary spectroscopic measurements, the SXR emissions allow for the calculation of the localW-concentrations using an ionization equilibrium neglecting transport. The latter assumption has been proven to be reasonable for W in the core (see [51]) and from the W-concentration the total, local radiated power densities can be derived using the W cooling factor [52]. In principle a similar (more direct) evaluation of the W density and radiation profiles could be performed using radiation profiles measured by bolometry. However it turned out that the bolometer measurements can be dominated by divertor and edge radiation, making the deconvolution of the core radiation less precise and more prone to artifacts. The deduced strong localized radiation peaking is very characteristic for so-called central impurity accumulation. In [53, 54] it has been found that impurity accumulation occurs when turbulent transport in the plasma core is weak, and the neoclassical transport becomes important. The cleaning effect of large turbulent core transport is not only based on diffusive effects, but also supported by a turbulent outward pinch for the impurities requiring steep temperature gradients [55, 56]. The radiation/heating balance in the core of the presented Pulse No: 81913 (Fig.5) reveals radiative cooling of similar size as the local heating power thereby decreasing the core T_e and flattening the T_e gradients leading to a feedback loop of decreasing transport and increasing radiation [49].

This investigation of the local power balance seems to be the key for understanding the accumulation process and the application of mitigation methods. Applying a sufficiently large gas

puff (10^{22} s^{-1}) decreases the edge temperatures and thereby the W source and the W penetration. Furthermore the increase of ELM frequency efficiently expelsW from the pedestal region [43]. Altogether this leads to a reduction of the W density at the pedestal top, which sets the boundary condition for the core W density. Keeping this level low allows to maintain large enough anomalous transport in the core suppressing the self-amplification of the central accumulation. On the other hand increasing the local heating power in the centre (see for example [57, 58, 24]) makes the core less vulnerable even at higher impurity/radiation levels.

3.5. RADIATIVE COOLING

With the change to the JET-ILW, a strong reduction of the C divertor radiation was expected (and eventually also found). In order to prepare for this situation, specifically in the presence of the enhanced NBI heating power, an elaborate program on radiative cooling using either N_2 or Ne was conducted in JET-C [59, 60]. Typical for these discharges was a moderate degradation of the confinement (see Fig.6) with increasing impurity injection. The transition from the type-I to the type-III ELM regime turned out to be the limitation in achieving a large ratio of divertor/X-point radiation over main plasma radiation with an H-factor close to 1.

Similar discharges were repeated in JET-ILWwith practically identical shape (2.5MA/2.7T) with the aim to characterize the differences between JET-C and JET-ILW [61]. As described above, the W contamination in the main plasma made operation at low fuelling difficult and high- ELMy H-mode at 2.5MA is restricted to fuelling levels higher than $0.9 \cdot 10^{22}$ Ds^{-1} in contrast to the lowest fuelling of $\approx 0.3 \cdot 10^{22}$ Ds^{-1} in JET-C related studies. Generally, the unseeded discharges in the ILWshow a lower radiation fraction and a lower Z_{eff} compared to their JET-C counterpart, when staying above the minimum fuelling level. The measurements confirm that as nitrogen is injected in the plasma, the divertor behaviour similar to the JET-C N_2-seeded discharges is recovered. In fact, partial divertor detachment is obtained at the N_2 seeding rate of $\approx 2.5–3.7 \cdot 10^{22}$ Ds^{-1} and with fuelling rate from 0.8 and $2.9 \cdot 10^{22}$ Ds^{-1} and the electron temperature is then reduced to ≈5eV. Different to JET-C, type-I ELMy plasmas exist in JET-ILWbelow the critical electron temperature deduced for type-III ELMs in JET-C at high density. In addition to increasing the radiative power and reducing the inter ELM power load, nitrogen seeding has been found to improve plasma energy confinement in high- ELMy H-modes by raising the pedestal density and temperature. This leads to H-factors only slightly below their JET-C counterparts as seen in Fig.6 a). A very good match is found if the density dependence is removed from the ITERH98(y,2) H-factor scaling, as shown in Fig.6b), since ne of seeded discharges tends to be higher in JET-ILW than JET-C for the same seeding level. The best N_2-seeded pulse in JET-ILW yielded ne/nGW Section 1 1 with $Z_{eff} \approx 1.5$.

This is the first time in JET that injection of impurities lead to an increase in global energy confinement. It is important to note that the increase in confinement stems from the pedestal and not from an improved energy and particle confinement in the core plasma, since density and temperature peaking remained unaffected. A similar correlation between nitrogen seeding rate and stored energy

has already been observed in AUG and is reported to be linked to a positive correlation between H-factor and Z_{eff} [48] which is not (yet) found with the JETILW.

The JET-ILW results strongly suggest that the carbon impurities played a role in the performance of the high-shape plasma scenario in JET-C. In JET-ILW plasmas the divertor radiative power and the pedestal confinement increase up to values similar to those in the deuterium fuelled JET-C counterparts, as the nitrogen seeding rate is increased. Once the maximumpedestal pressure has been achieved with nitrogen seeding, a further raise in seeding level leads to a decrease in density and a weaker decrease in temperature, very similar to the behaviour of plasmas in JET-C with N_2-seeding. These observations indicate that C level and associated radiation may have been a hidden parameter in the JET-C confinement behaviour in high-shape fuelled discharges, and that the injection of N_2 partially recovers this effect. A direct consequence of the increased edge stability resulting in higher confinement and lower ELM frequency is the tendency for an un-stationary behaviour similar to that shown for the seeded case in the Fig.5. It is, however, important to note that high- ELMy H-modes were not stationary in JET-C either. In fact, ICRH was added to neutral-beam heating as an integral part of the scenario for control of density peaking and sawteeth [62, 63]. In the JETILW discharge, first test with ICRH heating in this scenario did not show any benefit so far, probably due to the lower available power and the additionally induced W source (see Sec.2.2).

Although the confinement improvement was found to be very robust in high δ discharges it could not be reproduced in low-δ configurations. The range of Z_{eff} values covered with the low-configuration was from 1.2 to 1.5 and thereby covering the important part of the range covered with high-δ plasmas (1.1–1.8). The reason for this different behaviour is not clear but it reflects to some extent the differences in confinement behaviour already observed in D-puffed discharges in JET-C. In course of this investigations on low- discharges, also vertical target configuration were tested, whereas in almost all other investigations the outer strike point was positioned on the horizontal bulk W target ('tile 5'). In terms of divertor geometry this configuration is much closer to the ITER configuration. Interestingly the W contamination in the main plasma was much reduced and the operational window seemed to extend to very low fuelling close to levels used in JET-C. Due to the limited amount of discharge time this beneficial behaviour could not be investigated in detail but it will be a top priority for the upcoming campaign in 2013.

3.6. CONFINEMENT STUDIES

A JET-ILW scenario confinement database has been constructed with over 400 baseline H-mode (Type I ELMs) and hybrid plasmas [64]. This database has been compared with a similar one which was establish in JET-C [65]. In JET-C, baseline ELMy Hmode plasmas achieved good normalised confinement with $H98 \approx 1$ in un-fuelled plasmas. High triangularity baseline plasmas could be fuelled up to the Greenwald density without confinement loss, whereas gas-fuelled low triangularity plasmas showed a degraded confinement. In JET-ILW increased fuelling was required to avoid W contamination (see above). Although there is insufficient overlap in high gas fuelling levels for the

JET-C and JET-ILW experiments, the data trend suggests that the low triangularity plasmas show a similar degradation of H98 with fuelling level in JET-ILW compared to JET-C. However, the confinement in JET-ILW high triangularity baseline plasmas is reduced by 10–30% over the entire fuelling range. The change in confinement in the high triangularity pulses is not due a change in plasma radiation. In the absence of carbon as a radiator, the divertor radiation is reduced in JET-ILW compared to JET-C, and in absence of strong W contamination, the core radiation in JET-ILW is similar or even lower than in JET-C.

The global normalised confinement of the hybrid plasmas in JET-ILW was comparable to that in JET-C for both low and high triangularity hybrid plasmas. In JET-C the achievable confinement was best at low or zero gas fuelling, where $H98 \leq 1.4$ was achieved for both low and high triangularity. In JET-ILW this was not achievable due to the need to mitigate W accumulation with gas fuelling. However at similar fuelling levels the confinement in low and high triangularity hybrid plasmas was similar in the JET-ILW experiments compared to the JET-C experiments.

The main reason for the confinement reduction in plasmas in the ILW is the reduction in pedestal pressure, which sets the boundary condition for the core and under stiff core profile conditions the global confinement is affected. In the hybrid plasmas, where also some loss of pedestal confinement was observed, it was compensated by a steepening of the core profiles, and as a consequence the global confinement approached that achieved in JET-C. In the absence of ion temperature measurements $T_i = T_e$ is assumed. This is justified by the relatively high plasma densities in baseline JET-ILW plasmas, such that the ion-electron heat exchange time is low compared to the energy confinement time - but this needs to be verified with actual T_i measurements when available. Obviously, the role of plasmas shaping and particular the triangularity in setting the edge stability has reduced in JET-ILW. The high triangularity plasmas are stronger affected by the change in wall material than the low triangularity plasmas. It seems that the change in the edge impurity composition has a stronger effect on the edge stability when the triangularity is increased. An increased Z_{eff} in the pedestal region leads to ion dilution and secondly affects edge current distribution. Replacing carbon with nitrogen as a divertor impurity indeed can affect the pedestal confinement indicating the importance of the role of the impurity composition (see Sec.3.5) specifically in high triangularity plasmas. The role of edge impurities on the pedestal stability remains to be studied, but the absence of C as an edge impurity seems to be a good candidate to explain the observed differences in JET-C and JET-ILW. Furthermore, the core profile stiffness can be affected by the core rotation and/or rotation gradients [66], which may have changed due to the different energy mix of the NBI particles. However no rotation profiles are available yet and a detailed study of core profile stiffness will be conducted as soon as measurements are available.

4. SUMMARY AND CONCLUSIONS

With first operation with the ITER-like wall in JET many results achieved in Alcator C-Mod and ASDEX Upgrade could be confirmed, but also new aspects due to ITER-like material were

unraveled. The first result achieved was the documentation of the strongly facilitated conditioning, allowing the device to be run throughout the campaign without glow discharge or any other surface conditioning. This is reflected also in the very reliable breakdown over a much larger density range compared with C PFCs. The reason for this very beneficial behavior can be found in the very low C and O content documented by spectroscopic and Z_{eff} measurements and low levels of retained gas which make control of the initial density much easier with ILW.. The absence of C as a radiator is also found during unmitigated disruptions, leading to a low fraction of radiated energy during the thermal quench. Consequently, rather high plasma temperatures prevail after the thermal quench resulting a very slow current decay, large reaction forces on the vessel and rather high localized power loads. The use of massive gas injection strongly increases the radiated energy as well as it reduces the reaction forces in both cases to levels observed in mitigated disruptions in JET-C. The D retention is reduced by at least a factor of 10 in all investigated scenarios, which is consistent with earlier estimations. The absolute amount of the retained D is being deduced in post mortem investigations of tiles recently retrieved from JET at the end of 2012. Comprehensive investigations have shown a significantly lower L-H threshold than in JET-C as well as distinct minimum density below which the threshold rises again different to results in JET-C but similar to earlier results in JET with the MK II - gasbox divertor configuration as well as from Alcator C-mod and ASDEX Upgrade. ICRH has proven a similar efficiency as NBI in L-Mode discharges however an increased level of W and Ni is observed during ICRH despite the higher central temperatures reached. The sources for this increase could not be identified yet but the temporal behaviour of the recovery of the impurity level after a Be evaporation hints to the fact that remote areas not directly exposed to large plasma fluxes strongly contribute to the impurity source. This observation is particularly important because it suggests that the in ITER the W ICRH induced W source will not play a dominant role since the whole main chamber is covered by Be. In addition, the distinctively different behaviour to the ASDEX Upgrade, where the antenna limiter itself was identified as the main source, provides useful information for antenna optimisation. As expected, the operational space in H-Mode was reduced compared to the operation of JET-C. Most importantly no H-Mode discharges could be performed with zero gas-puffing. Although this denies the access to low density edge conditions, it provides a focus on operation schemes accessible with gas-puffing which will be also a prerequisite for ITER and DEMO. The counter measures developed earlier in ASDEX Upgrade for the prevention ofWaccumulation could be mostly confirmed, although the ICRH was not yet able (due to technical constraints) to provide a significant reduction of the centralWconcentration in H-Mode. The most striking effect with the JET-ILW was the lower pedestal confinement observed in comparable discharges. There is no evidence that this is caused by W radiation. On the contrary the discharges showing a good (pedestal) confinement tend to have a higher W concentration and W bulk radiation, due to improved particle confinement than similar discharges with lower confinement. At the moment there is no theory or modeling based explanation for this degradation. An important experimental observation comes from nitrogen seeding experiments which allow to

recover most of the confinement in high discharges by leading to increased pedestal temperatures. Since nitrogen radiates at similar temperatures as carbon it may play to role of a surrogate for the missing C in the plasma edge.

In its first year of operation, the JET ITER-likeWall experiment has achieved important results for the operation of ITER. Although not all of the results provide a positive scaling towards ITER, none of them is seen as a show stopper. Some of the surprising results even may give rise to new theoretical insight in confinement physics. As part of the stepwise approach foreseen from the very beginning of the ILW the next campaigns will concentrate on the expansion and exploration of the full operational range of JET, allowing more than 30MW of auxiliary heating power.

ACKNOWLEDGEMENT

The authors wants to thank the colleagues from Jet-EFDA for providing their latest results. This work was supported by EURATOM and carried out within the framework of the European Fusion Development Agreement. The views and opinions expressed herein do not necessarily reflect those of the European Commission.

REFERENCES

[1]. J. Pamela, G. Matthews, V. Philipps, and R. Kamendje, Journal of Nuclear Materials **363-365**, 1 – 11 (2007).

[2]. G. Matthews, P. Edwards, T. Hirai, M. Kear, A. Lioure, et al., Physica Scripta **T128**, 137–143 (2007).

[3]. R. Pitts, S. Carpentier, F. Escourbiac, T. Hirai, V. Komarov, et al., accepted for publication in Journal of Nuclear Materials, http://dx.doi.org/10.1016/j.jnucmat.2011.01.114 (2011).

[4]. C. Ruset, E. Grigore, H. Maier, R. Neu, X. Li, et al., Physica Scripta **T128**, 171–174 (2007).

[5]. T. Hirai, H. Maier, M. Rubel, P. Mertens, R. Neu, et al., Fusion Engineering and Design 82(15-24), 1839– 1845 (2007), Proceedings of the 24th Symposium on Fusion Technology - SOFT-24.

[6]. H. Maier, R. Neu, H. Greuner, B. B¨oswirth, M. Balden, et al., Physica Scripta **T138**, 014031 (2009).

[7]. P. Mertens, Physica Scripta 2011 **T145** , 014002 (2011).

[8]. G. Matthews, M. Beurskens, S. Brezinsek, M. Groth, E. Joffrin, et al., Physica Scripta **T145**, 014001 (2011).

[9]. V. Riccardo, M. Firdaouss, E. Joffrin, G. Matthews, P. Mertens, et al., Physica Scripta 2009 **T138**, 014033 (2009).

[10]. G. Arnoux et al., submitted Review of Scientific Instruments (2012).

[11]. P. de Vries et al., submitted to Nuclear Fusion (2012).

[12]. H. Kim, A. Sips, , W. Fundamenski, and EFDA-JET contributors, Nuclear Fusion **52**, 103016 (2012).

[13]. S. Brezinsek, S. Jachmich, M. Stamp, A. Meigs, J. Coenen, et al., Journal of Nuclear Materials (0), – (2013).
[14]. K. Krieger, S. Brezinsek,M. Reinelt, S. Lisgo, J. Coenen, et al., Journal of NuclearMaterials (0), – (2013).
[15]. J. Coenen, M. Sertoli, S. Brezinsek, I. Coffey, R. Dux, et al., submitted to Nuclear Fusion (2012).
[16]. K. Behringer, H. Summers, B. Denne, M. Forrest, and M. Stamp, Plasma Physics and Controlled Fusion **31**, 205– 2099 (1989).
[17]. D. Borodin, M. Stamp, A. Kirschner, C. Bjrkas, S. Brezinsek, et al., Journal of Nuclear Materials (0), –(2013).
[18] G. van Rooij, J. Coenen, L. Aho-Mantila, M. Beurskens, S. Brezinsek, et al., IAEA FEC conference, San Diego , EX/P5–05 (2012).
[19]. M. Laengner et al., accepted for publication in Journal of Nuclear Materials (2012).
[20]. R. Dux, V. Bobkov, A. Herrmann, A. Janzer, A. Kallenbach, et al., Journal of Nuclear Materials **390–391**, 858–863 (2009).
[21]. D. van Eester et al., EPS Conf. Stockholm (2012).
[22]. T. Pütterich, R. Neu, R. Dux, A. D. Whiteford, M. G. O'Mullane, et al., Plasma Physics and Controlled Fusion **50** (8), 085016 (2008).
[23]. R. Neu, R. Dux, A. Geier, H. Greuner, K. Krieger, et al., Journal of Nuclear Materials **313–316**, 116–126 (2003).
[24]. M. Valisa, L. Carraro, I. Predebon,M. Puiatti, C. Angioni, et al., Nuclear Fusion **51**(3), 033002 (2011).
[25]. V. Bobkov, G. Arnoux, S. Brezinsek, J. Coenen, L. Colas, et al., Journal of Nuclear Materials (0), – (2013).
[26]. P. C. de Vries, G. Arnoux, A. Huber, J. Flanagan,M. Lehnen, et al., Plasma Physics and Controlled Fusion **54**(12), 124032 (2012).
[27]. M. Groth, S. Brezinsek, P. Belo, G. Corrigan, D. Harting, et al., Journal of NuclearMaterials (0), – (2013).
[28]. M. Lehnen et al., submitted to Nuclear Fusion (2012).
[29]. V. Philipps, T. Loarer, H. Esser, S. Vartanian, U. Kruezi, et al., Journal of Nuclear Materials (0), – (2013).
[30]. T. Loarer, S. Brezinsek, V. Philipps, J. Bucalossi, D. Douai, et al., Journal of Nuclear Materials (0), –(2013).
[31]. S. Brezinsek et al., submitted to Nuclear Fusion (2012).
[32]. S. Brezinsek, W. Fundamenski, T. Eich, J. Coad, K. McCormick, et al., accepted for publication in Journal of Nuclear Materials (2011).
[33]. J. Roth, E. Tsitrone, A. Loarte, T. Loarer, G. Counsell, et al., Journal of Nuclear Materials **390–391**, 1–9 (2009).

[34]. K. Sugiyama, M. Mayer, V. Rohde, M. Balden, T. Durbeck, et al., Nuclear Fusion **50**(3), 035001 (8pp) (2010).
[35]. V. Philipps et al., Journal of Vacuum Science Technology A **11**(2), 437 (1993).
[36]. C. Maggi et al., subm. to Plasma Physics and Controlled Fusion (2012).
[37]. Y. R. Martin, T. Takizuka, and the ITPA CDBM H-mode Threshold Database Working Group, Journal of Physics: Conference Series **123**(1), 012033 (2008).
[38]. J. Snipes et al., Plasma current dependence of the H-mode threshold low density limit on Alcator C-Mod, in Europhysics Conf. Abstracts (CD-ROM)Proc. 35th EPS Plasma Physics Conf. (Hersonissos, Greece), page P1.074, EPS, 2008.
[39]. F. Ryter, T. Pütterich, M. Reich, A. Scarabosio, E. Wolfrum, et al., Nuclear Fusion **49**, 062003 (2009).
[40]. R. Neu, A. Kallenbach,M. Balden, V. Bobkov, J. Coenen, et al., Journal of NuclearMaterials (0), – (2013).
[41]. E. Joffrin et al., submitted to Nuclear Fusion (2012).
[42]. R. Neu, R. Dux, A. Kallenbach, T. Pütterich, M. Balden, et al., Nuclear Fusion **45**(3), 209–218 (2005).
[43]. R. Dux, A. Janzer, T. P¨utterich, and ASDEX Upgrade Team, Nuclear Fusion **51**(5), 053002 (2011).
[44]. G. Saibene et al., Nuclear Fusion **39**, 1133 (1999).
[45]. E. de la Luna et al., submitted to Nuclear Fusion (2012).
[46]. J. Hobirk, F. Imbeaux, F. Crisanti, P. Buratti, C. D. Challis, et al., Plasma Physics and Controlled Fusion 54(9), 095001 (2012).
[47] M. Baruzzo et al., 54th APS annual meeting, Providence, RI, USA (2012).
[48]. J. Schweinzer, A. Sips, G. Tardini, P. Schneider, R. Fischer, et al., Nuclear Fusion **51**(11), 113003 (2011).
[49]. T. Pütterich et al., submitted to Nuclear Fusion (2012).
[50]. J. Wesson, Nuclear Fusion 37, 577 (1997).
[51]. K. Asmussen, K. B. Fournier, J. M. Laming, R. Neu, J. F. Seely, et al., Nuclear Fusion **38** (7), 967–986 (1998).
[52]. T. Pütterich, R. Neu, R. Dux, A. Whiteford, M. O'Mullane, et al., Nuclear Fusion **50** (2), 025012 (9pp) (2010).
[53]. R. Dux, C. Giroud, R. Neu, A. G. Peeters, J. Stober, et al., Journal of Nuclear Materials **313–316**, 1150– 1155 (2003).
[54]. R. Dux, R. Neu, A. G. Peeters, G. Pereverzev, A. M¨uck, et al., Plasma Physics and Controlled Fusion **45** (9), 1815–1825 (2003).
[55]. M. Puiatti et al., Physics of Plasmas **13**, 042501 (2006).
[56]. M. Sertoli, C. Angioni, R. Dux, R. Neu, T. Pütterich, et al., Plasma Physics and Controlled Fusion **53**(3), 035024 (2011).

[57]. R. Neu, R. Dux, A. Geier, A. Kallenbach, R. Pugno, et al., Plasma Physics and Controlled Fusion **44** (6), 811–826 (2002).
[58]. J. E. Rice, P. Bonoli, E. Marmar, S. Wukitch, R. L. Boivin, et al., Nuclear Fusion **42**, 510–519 (2002).
[59]. G.Maddison, C. Giroud, G.McCormick, J. Alonso, B. Alper, et al., Nuclear Fusion **51**(4), 042001 (2011).
[60]. C. Giroud et al., Nuclear Fusion **52**, 063022 (2012).
[61]. C. Giroud et al., submitted to Nuclear Fusion (2012).
[62]. G. Saibene, R. Sartori, A. Loarte, D. J. Campbell, P. J. Lomas, et al., Plasma Physics and Controlled Fusion **44** (9), 1769–1800 (2002).
[63]. M. F. F. Nave, J. Rapp, T. Bolzonella, R. Dux, M. J. Mantsinen, et al., Nuclear Fusion **43** (10), 1204–1213 (2003).
[64]. M. Beurskens et al., submitted to Nuclear Fusion (2012).
[65]. M. Beurskens, L. Frassinetti, C. Challis, T. Osborne, P. Snyder, et al., Nuclear Fusion **53** (1), 013001 (2013).
[66]. P. Mantica et al., Physical Review Letters **107**, 135004 (2011).
[67]. J. Buccalossi et al., EPS Conf. Stockholm (2012).

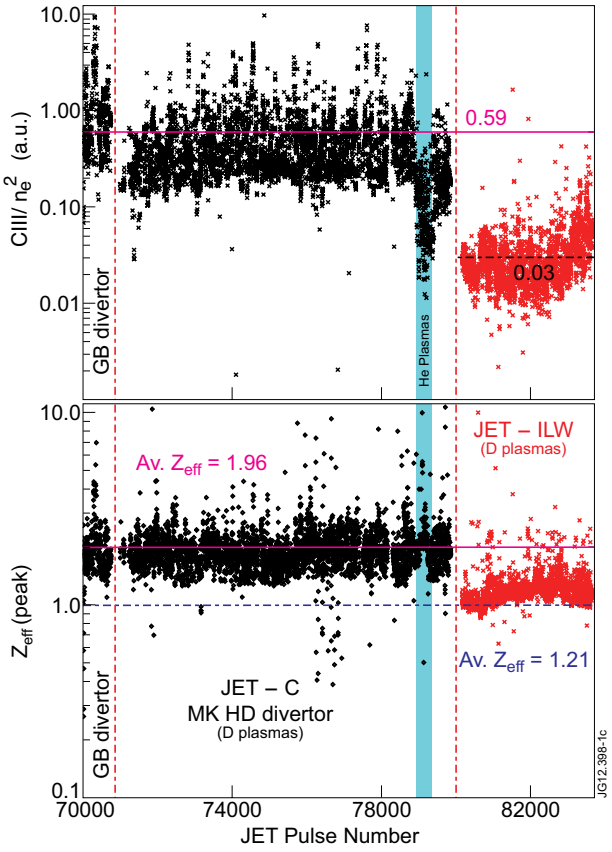

Figure 1: Reduction of carbon influx and Z_{eff} after the transition from carbon PFCs to Be andWPFCs.

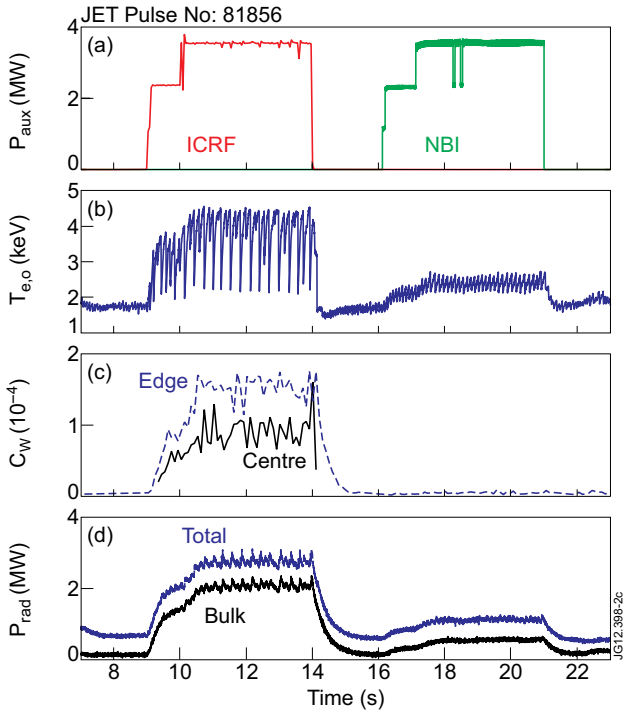

Figure 2: Behaviour of W content and bulk radiation in the L-Mode JET Pulse No: 81856 ($B_t = 2.55T, I_p = 2.5MA$).

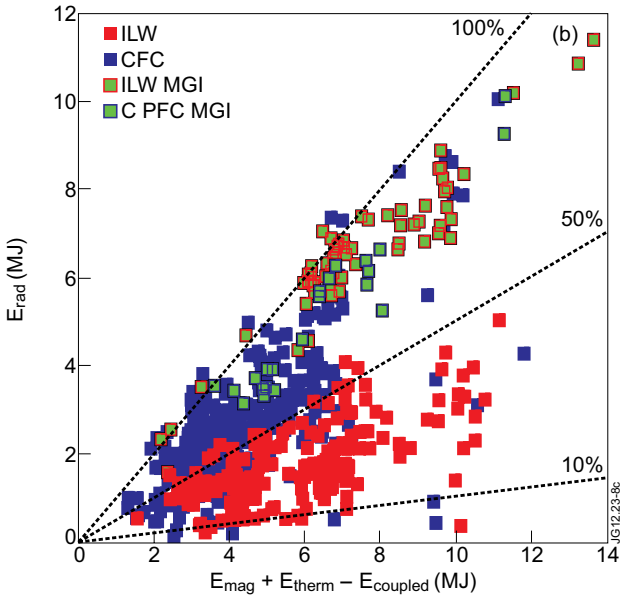

Figure 3: Radiated energy during the current quench of (un-)mitigated disruption in JET-C and JET-ILW versus the available thermal and magnetic energy (the energy coupled back into the toroidal conductors is subtracted).

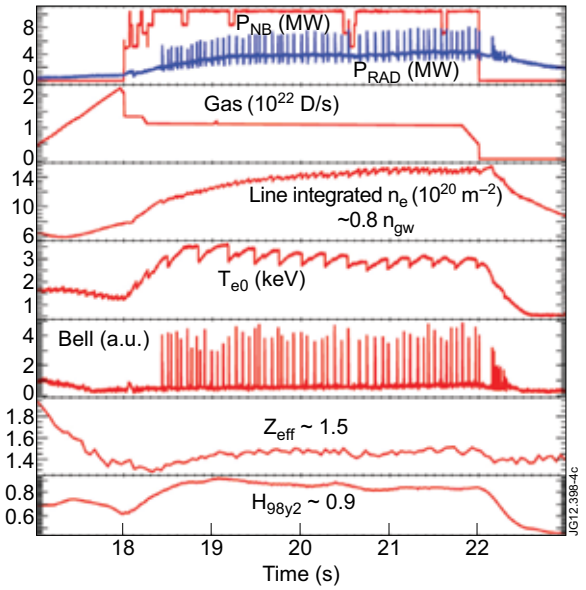

Figure 4: Stable H-mode discharge in JET-ILW with I_p = 2.0MA, B_t = 2.1T [67].

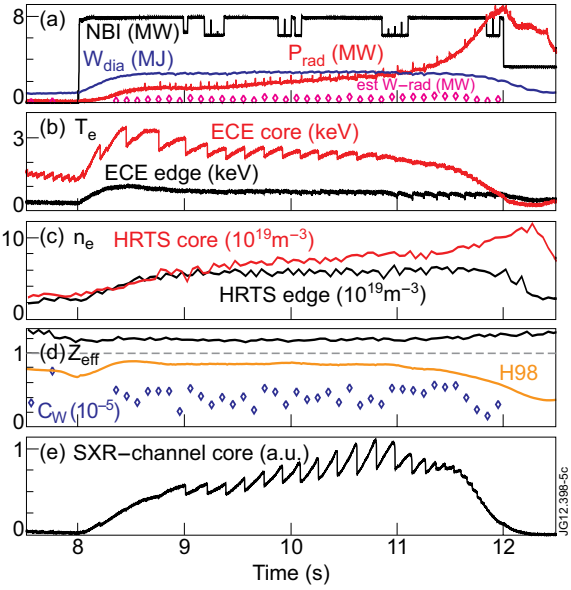

Figure 5: Evolution of W-accumulation in a I_p = 2.0MA, B_t = 2.1T H-Mode discharge.

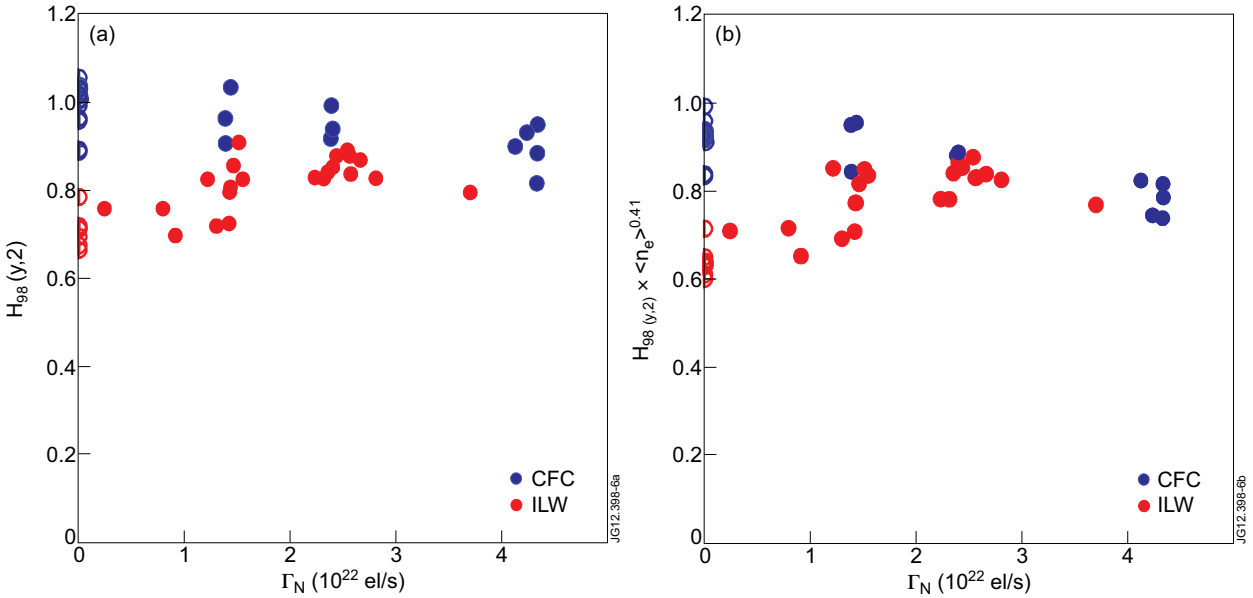

Figure 6: Normalized confinement versus N_2-seeding rate: a) compared to the H98(y,2) scaling and b) with the density dependence removed from the H98 scaling.